

Amplitude Analysis of the decay $B^+ \rightarrow \pi^+ K^- K^+$

I. Bediaga¹, M. Cruz Torres¹, C. Göbel², J. M de Miranda¹, F. Rodrigues³, V. Salustino²

¹ Centro Brasileiro de Pesquisas Físicas (CBPF), Brazil

² Pontifícia Universidade Católica do Rio de Janeiro (PUC-Rio), Brazil

³ Universidade Federal do Rio de Janeiro (UFRJ-Xerem), Brazil

Workshop on multibody charmless B-hadron decays



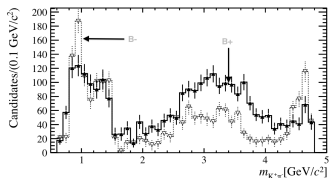
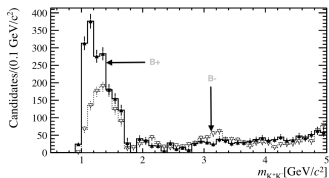
June 7, 2018

Motivation

- Large integrated CP asymmetry reported by the LHCb for this channel.

$$A_{CP}(B^\pm \rightarrow \pi^\pm K^+ K^-) = -0.123 \pm 0.017 \pm 0.012 \pm 0.007$$

Significance: 5.6σ

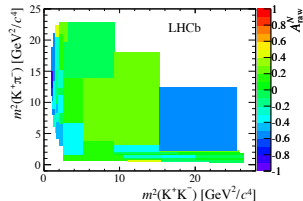


Phys. Rev. Lett. 112, 011801 (2014)/LHCb-ANA-2013-052

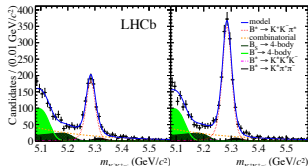
Phys. Rev. D 90, 112004 (2014)/LHCb-ANA-2014-050

(CBPF)

- In fact large asymmetries were localized in regions of the phase space.



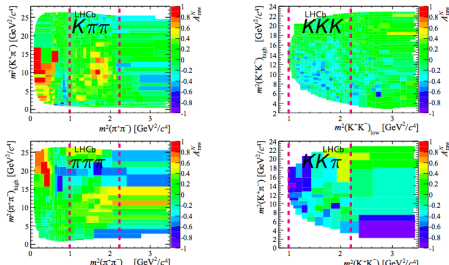
- re-scattering region in $m_{KK} < 1.5$ GeV/c²



$$A_{\text{Raw}} = -0.328 \pm 0.028 \pm 0.029 \pm 0.007$$

CP asymmetry in the phase space

- Doing a zoom at the low mass region for the four channels:



- This region precisely correspond to the expected rescattering region $\pi\pi \leftrightarrow KK$ ($1-1.5$ GeV/c^2).

Large asymmetries found in this particular region for the four channels:

$$(a) B^\pm \rightarrow \pi^\pm \pi^+ \pi^-$$

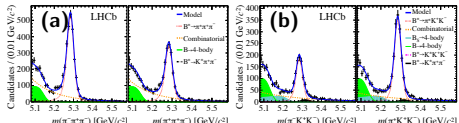
$$\mathcal{A}_{CP} = +0.172 \pm 0.021 \pm 0.015 \pm 0.007$$

$$(b) B^\pm \rightarrow K^\pm K^+ \pi^-$$

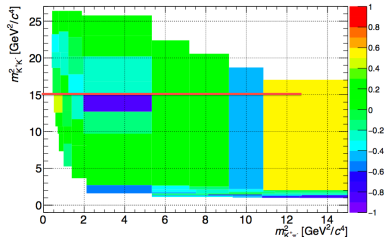
$$\mathcal{A}_{CP} = -0.328 \pm 0.028 \pm 0.029 \pm 0.007$$

Notice the interesting feature that the asymmetry in this low mass region has opposite sign for:

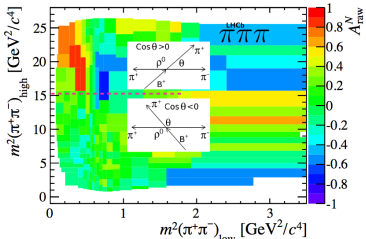
$B \rightarrow K\pi\pi$ and $B \rightarrow KKK$ and for
 $B \rightarrow \pi\pi\pi$ and $B \rightarrow KK\pi$



CP asymmetry in the phase space



Asymmetries behaviour change at the middle line.



- We can divide these regions by de cosine of the helicity angle:
 $\cos\theta > 0$ and $\cos\theta < 0$
- The exploration of these regions in detail could give us information about the possible sources of these asymmetries.

Motivation

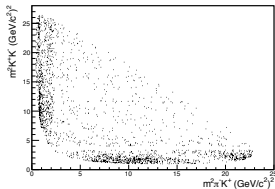
- The origin of this asymmetry is not clear but due to the rich dynamic structures.

These can be the result of different sources like:

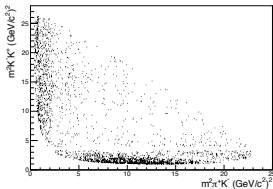
- $\pi\pi \leftrightarrow KK$ rescattering of the final states particles via strong interaction.
- Interference of the intermediate resonant states with different weak and strong phases.
- Direct CP Violation on intermediate states.

In order to understand the origin of these asymmetries and the rich structures present in the Dalitz plot it is necessary to perform an Amplitude Analysis.

B^-



B^+



- Amplitude Analysis for this channel is being performed for the first time.

- Very challenging:

- Combined fit for B^+ and B^- allowing for CPV.
- Difficulties with the amplitude model.

- High Asymmetries observed clearly.

Analysis Strategy

- Event selection and mass fit to define the signal region and determine N_{sig} and N_{bkg} .
- Construction of the signal efficiency model.
- Construction of the models for the background sources contributing in the signal region.
- Build the Isobar Model through a systematic procedure.
- Dalitz plot fit using Laura++.

Analysis still in review by the collaboration ⇒ Unofficial results.

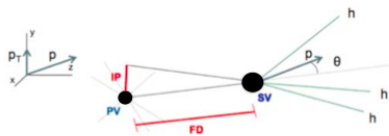
Event Selection

- **Online:** Selection thanks to the trigger system.

- **High-Level trigger (software):** Is based in algorithms that perform partial (HLT1) and full reconstruction of all tracks (HLT2).

Some of the variables used.

- P_T of the mother and the daughter particles.
- FD and FD χ^2 .
- IP of the mother and the daughter particles
- IP χ^2 of the mother and the daughter particles.
- χ^2 of the secondary vertex.
- Dedicated variables for the particle identification between π and K .



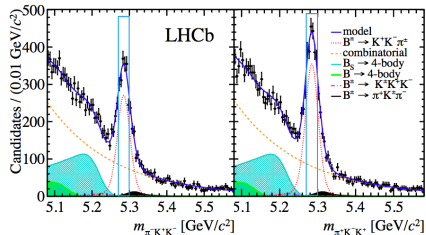
- Variables that are good at discriminating signal from background events.
 - In a second stage a multivariate analysis was performed.
 - We also exclude events of B^+ decaying to charm: $D^0 \rightarrow \pi^+ K^-$, $D^0 \rightarrow K^- K^+$.

1D mass fit

- Signal PDF parametrized by a Gaussian + 2 Crystal Ball (CB).
- Combinatorial background → exponential function.
- Peaking bkg → 2CB + 1 Gaussian.
- Partially reconstructed 4-Body decays are modelled using an Argus function convoluted with a Gaussian resolution.

For the Dalitz plot fit:

- Models for the relevant background contributions are constructed.
- Signal to background ratio given as input.



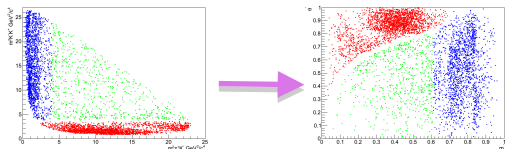
Signal region: $|5283 - m_B| < 17\text{MeV}$.

- Signal: ~ 74%
- Comb. Bkg ~ 22%
- 4-Body ~ 0.25%
- Peaking KKK ~ 0.12%
- Peaking kppi ~ 2.67%

Acceptance correction for B^+ and B^-

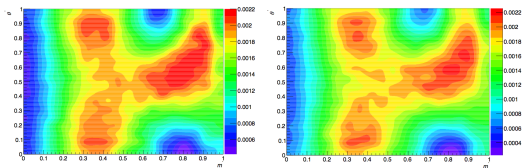
For the efficiency and background models we use the concept of the *Square Dalitz plot* representation

$$dm_{12}^2 dm_{23}^2 \rightarrow |\det J| dm' d\theta'$$



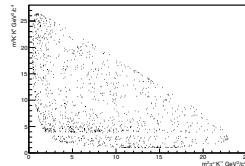
- The acceptance maps were generated with kinematics cut, with PID efficiency weights applied (PidCalib) and with L0-trigger efficiency correction.
- They were normalized to the distribution of generated events and smoothed out by a CubicSpline function.

Total signal efficiency
models separated by
charge:

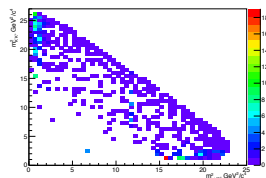


Background models same model used for B^+ and B^-

- Combinatorial background ($\sim 22\%$):
constructed using the right side events: $5400 < B_- m < 5500 \text{ MeV}/c^2$

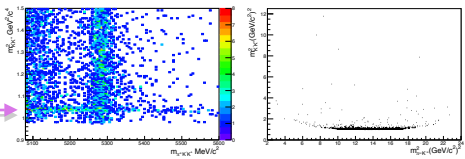


- Peaking background ($\sim 2.6\%$): MC simulated $B^+ \rightarrow \pi^+ \pi^- K^+$ sample mis-ID as $B^+ \rightarrow \pi^+ K^- K^+$, re-weighted event by event to bring the $B^+ \rightarrow \pi^+ \pi^- K^+$ Dalitz plot structure based on the BaBar model is used (PRD 78 (2008) 012004).



- Background contamination due to prompt produced $\phi(1020)$ mesons ($\sim 0.6\%$).

A Toy MC for $\phi(1020)$ decaying into $K^+ K^-$ is generated, imposing to not have angular signature.



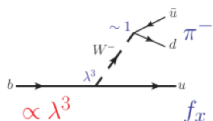
Dalitz plot Fit (Unofficial results)

Exploring the charged $B^+ \rightarrow \pi^+ K^- K^+$ decay :

Main Feynman diagrams are

Tree-level:

$$(b \rightarrow u) \sim |\mathbf{V}_{ub}|$$



- Expected contributions on the $\pi^+ K^-$ system:

$K^{*0}(892)$, $K^{*0}(1430)$, NR, kappa,..

- Expected contributions on the $K^- K^+$ system:

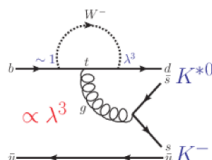
f_0 , f_2 , NR,...

- Notice that no $s\bar{s}$ resonances are expected e.g ϕ

- $f_0(980)$ might be contributing but not with a large fraction expected (is suppressed as it has almost $s\bar{s}$ composition).

Penguin:

$$(b \rightarrow (u, c, t) \rightarrow d) \sim |\mathbf{V}_{td}|$$



$$\begin{pmatrix} 1 - \lambda^2/2 & \lambda & \mathbf{A}\lambda^3(\rho - i\eta) \\ -\lambda & 1 - \lambda^2/2 & \mathbf{A}\lambda^2 \\ \mathbf{A}\lambda^2(1 - \rho - i\eta) & -\lambda\lambda^2 & 1 \end{pmatrix}$$

- At quark level two interfering amplitudes: *Tree* & *Penguin*, with different phases.

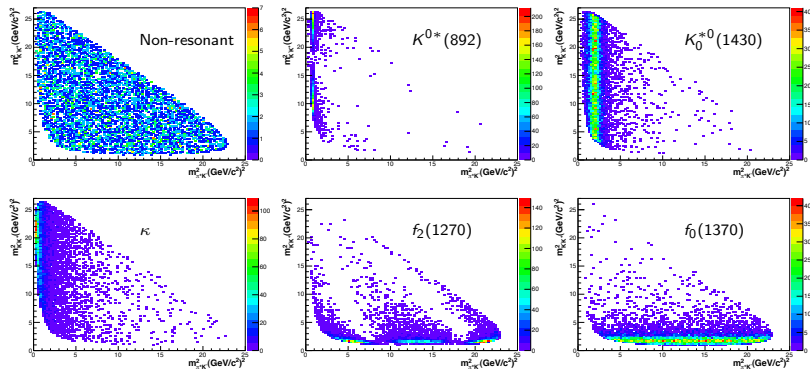
- Dominated by resonant intermediate states, which signatures can be inspected in the so-called *Dalitz plot*.

Resonances simulation in the $B^+ \rightarrow \pi^+ K^- K^+$ Dalitz plot

⇒ Possible resonance contributions are expected in two systems:

- $\pi^+ K^-$ system (horizontal axis)
- $K^- K^+$ system (vertical axis)

Simulation of resonances without the presence of any other resonance and non-resonant contribution in the phase space:



Dalitz plot Isobar fit strategy

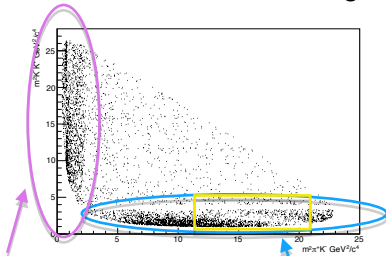
From the Isobar model the total signal amplitude for B^+ and B^- is defined as:

$$\mathcal{A}(\mathbf{m}_{K\pi}^2, \mathbf{m}_{KK}^2) = \sum_j c_j \mathcal{M}_{Rj}(\mathbf{m}_{K\pi}^2, \mathbf{m}_{KK}^2),$$

where $c_j = (x + \Delta x) + i(y + \Delta y)$ and $\bar{c}_j = (x - \Delta x) + i(y - \Delta y)$ is the complex coefficient for a given resonance decay mode j . Δx_j and Δy_j parametrize the CPV in the decay.

- We perform the DP fit separated by charge.
- We take as our references the $K^{0*}(892)$ resonances with x fixed in 1, y and Δy fixed in 0 and Δx is let free to float.
- The results are presented in polar coordinates, then $(x \pm \Delta x) + i(y \pm \Delta y)$ is converted to the form $a^\pm e^{i\delta^\pm}$
- The Software of analysis is [Laura++](#).

$B \rightarrow KK\pi$ DP for both charges



$K\pi$ system:

$K^{*0}(892)$, $K^{*0}(1430)$,

NR, kappa,...

KK system:

f_0 , f_2 , NR, ...

Resonances lineshapes tested:

Baseline: In general, relativistic Breit-Wigner.

Alternatives:

Non resonant based on “Tobias model” I.

Bediaga et al, Phys. Rev. D92, 054010(2015)

$\pi\pi \leftrightarrow KK$ Rescattering J. R. Pelaéz and F. J. Ynduráin,
PhysRev. D71, 074016(2005)

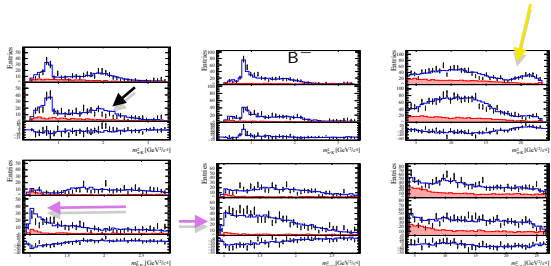
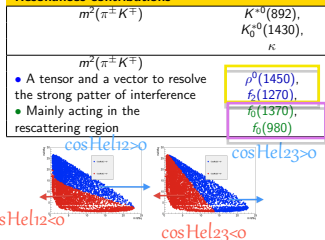
- Three family of fits were tested
- Classic model: Only known resonance and lineshapes were used. Baseline lineshape: RBW
- Including alternative parametrizations: Tobias NR and focus on the π^+K^- axis.
- Inclusion of a well tested rescattering amplitude: Pelaez 2005. Focus on the rescattering region- K^-K^- axis.

Dalitz plot fits

Classic Model

($-2\log \mathcal{L} = -9564$)

Resonances contributions



We find:

- 3 components to describe the structures on $m_{\pi^+ K^-}^2$ and 4 components for $m_{K^- K^+}^2$
- $\rho(1450)$ performs very well on parameterizing the high mass region on $m_{\pi^+ K^-}^2$ (strong pattern of interference)
- Large CP asymmetry attributed to $f_0(980)$ and $f_0(1370)$
- Both components mainly acting in the expected rescattering region.

Model 1-Improving the parametrization in $m_{\pi^+ K^-}^2$ projection

Model 1 \Rightarrow Focus in improving the πK system:

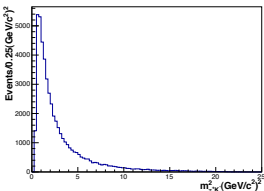
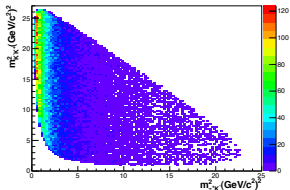
- **Tobias non-resonant function**

[Phys. Rev. D92.054010,2015] instead of κ

- Is a phenomenological description that gives more importance to the region of low-energy production of the final state particles.

$$T_{nr}(m_{\pi^+ K^-}^2) = \left(1 + \frac{m_{\pi^+ K^-}^2}{\Lambda^2}\right)^{-1},$$

where Λ was set to 1 GeV.



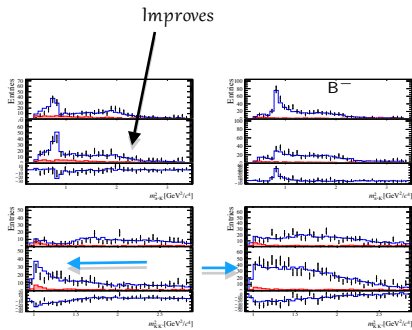
Dalitz plot fits

Model 1 ($-2\log\mathcal{L} = -9584$)

Resonances contributions

$m^2(\pi^\pm K^\mp)$	$K^{*0}(892),$ $K_0^{*0}(1430),$ Tobias NR
Replacing κ	
$m^2(\pi^\pm K^\mp)$	$\rho^0(1450),$ $f_2(1270),$ $f_0(1370),$ $f_0(980)$

- A tensor and a vector to resolve the strong pattern of interference
- Mainly acting in the rescattering region



- Introduction of Tobias NR instead of κ .
- Overall the DP fit is improved, specially in the $\pi^+ K^-$ system.
- Still Large asymmetries observed for $f_0(980)$ and $f_0(1370)$.
- Still large contribution attributed to $f_0(980)$.

Model 2- Dedicated parametrization for the rescattering region

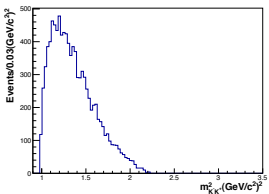
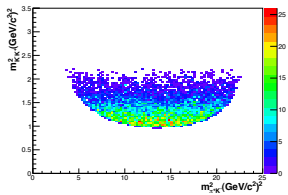
$$\text{Amplitude} = \sqrt{1 - (\eta_0^{(0)})^2} e^{2i\delta_0^{(0)}}$$

$$\cot \delta_0^{(0)}(s) = c_0 \frac{(s - M_s^2)(M_f^2 - s)}{M_f^2 s^{1/2}} \frac{|k_2|}{k_2^2}, \quad k_2 =$$

$$\frac{\sqrt{s - 4m_K^2}}{2};$$

$$\eta_0^{(0)} = 1 - \left(\epsilon_1 \frac{k_2}{s^{1/2}} + \epsilon_2 \frac{k_2^2}{s} \right) \frac{M'^2 - s}{s}.$$

- Rescattering amplitude for a region where no large resonance contributions are expected but the largest CP violation was measured. Using Pélaez *et al* parametrization (PhysRev. D71, 074016(2005)).



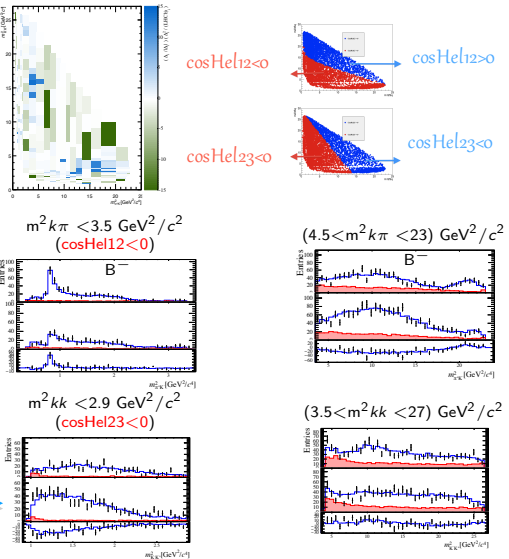
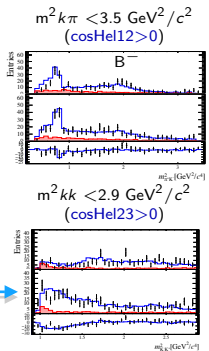
Model 2- Dedicated parametrization for the rescattering region

• Model 2: Using rescattering amplitude Pelaez 2005

[NLL -9564]	Fit fraction (%)		Magnitude and phase coefficients				A_{CP} (%)
Component	B^+	B^-	a_i^+	$\delta_i^+ [^\circ]$	a_i^-	$\delta_i^- [^\circ]$	
$K^{*0}(892)$	5.7 ± 1.1	10.0 ± 1.4	0.94 ± 0.04	0 ± 0	1.06 ± 0.04	0 ± 0	12.4 ± 8.7
$K_0^{*0}(1430)$	3.5 ± 0.9	5.9 ± 1.4	0.74 ± 0.09	-176 ± 10	0.82 ± 0.09	136 ± 11	10.6 ± 14.9
$TobiasNR_Kpi$	30.9 ± 4.4	34.3 ± 3.7	2.19 ± 0.13	-138 ± 7	1.97 ± 0.12	166 ± 6	-10.6 ± 5.3
$\rho^0(1450)$	29.0 ± 4.9	32.9 ± 4.6	2.12 ± 0.28	-175 ± 10	1.93 ± 0.24	141 ± 9	-9.5 ± 23.6
$f_2(1270)$	4.8 ± 1.2	11.1 ± 2.0	0.86 ± 0.16	-104 ± 11	1.12 ± 0.15	-128 ± 9	25.3 ± 27.0
Rescattering	23.8 ± 4.1	6.6 ± 0.9	1.92 ± 0.26	-52 ± 7	0.87 ± 0.08	-84 ± 21	-66.3 ± 10.7
Fit Fraction Sum	97.6	100.9					

- Rescattering parametrization used instead of $f_0(980)$ and $f_0(1370)$
- The rescattering component absorbs the negative CP asymmetry observed before on $f_0(980)$ and $f_0(1370)$.
 - The NLL went to a higher value than previous model (Model 1)
- We also performed the fit with rescattering parameters free, no substantial change observed.
- Several other functions were also tested as possible rescattering parametrization, no better result than the Pelaez 2005 was obtained.

Including Rescattering parametrization Pelaez 2005



Model 3: Adding the $\phi(1020)$ resonance : PROPOSED BASELINE MODEL

● Model 3: Adding $\phi(1020)$ resonance to Model 2.

[NLL -9573]	Fit fraction (%)		Magnitude and phase coefficients				A_{CP} (%)
Component	B^+	B^-	a_i^+	$\delta_i^+ [^\circ]$	a_i^-	$\delta_i^- [^\circ]$	
$K^{*0}(892)$	5.7 ± 0.6	10.0 ± 1.2	0.94 ± 0.04	0 ± 0	1.06 ± 0.04	0 ± 0	12.5 ± 8.7
$K_0^{*0}(1430)$	3.5 ± 0.8	5.9 ± 1.2	0.74 ± 0.09	-176 ± 10	0.82 ± 0.09	136 ± 11	10.5 ± 14.9
<i>TobiasNR_Kpi</i>	30.9 ± 2.0	34.1 ± 2.5	2.19 ± 0.13	-138 ± 7	1.97 ± 0.12	166 ± 6	-10.7 ± 5.3
$\rho^0(1450)$	29.5 ± 1.5	32.4 ± 1.9	2.14 ± 0.11	-175 ± 10	1.91 ± 0.10	140 ± 13	-11.0 ± 4.4
$f_2(1270)$	4.7 ± 0.9	11.2 ± 1.3	0.85 ± 0.09	-106 ± 11	1.13 ± 0.08	-128 ± 11	27.2 ± 10.2
Rescattering	23.7 ± 1.1	6.5 ± 0.8	1.92 ± 0.09	-57 ± 12	0.86 ± 0.07	-81 ± 15	-66.7 ± 3.8
$\phi(1020)$	0.2 ± 0.2	0.4 ± 0.2	0.20 ± 0.07	-53 ± 23	0.22 ± 0.06	108 ± 33	10.1 ± 43.8
Fit Fraction Sum	98.3	100.5					

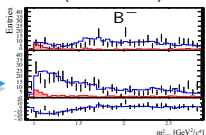
- Even when the decay $B^\pm \rightarrow \phi\pi^\pm$, $\phi \rightarrow K^+K^-$ is highly suppressed, it was established a upper limit for the corresponding branching fraction: $\mathcal{B}(B^\pm \rightarrow \phi\pi^\pm) < 1.5 \times 10^{-7}$ ([Phys. Letters B 728 \(2014\) 85](#)).
- Motivated by the poor fit in the region near the threshold K^+K^- , the possible contribution of this narrow resonance was tested.
- Fit fraction contribution found to be very small as expected, magnitudes found with 3σ significance.
- The solution of the other components remains pretty similar to Model 2 with an improvement in the NLL.

Model 3: Adding $\phi(1020)$ as component

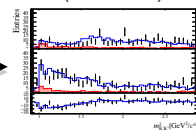
-Comparison:

- Model 2: $\rho(1450)$, $f_2(1270)$, rescattering (first row)
- Model 3: $\rho(1450)$, $f_2(1270)$, rescattering + $\phi(1020)$ (second row)

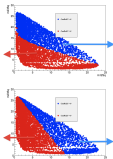
$$m^2 k\pi < 3.5 \text{ GeV}^2/c^2 \\ (\cos\text{Hel}12 > 0)$$



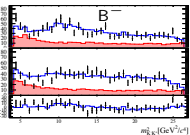
$$m^2 kk < 2.9 \text{ GeV}^2/c^2 \\ (\cos\text{Hel}23 > 0)$$



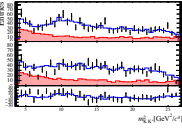
A slight improvement in the projections is observed.



$$(4.5 < m^2 k\pi < 23) \text{ GeV}^2/c^2$$

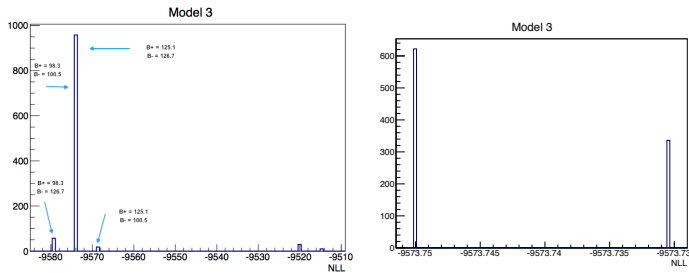


$$(3.5 < m^2 kk < 27) \text{ GeV}^2/c^2$$



Negative likelihood profile

- 2000 fits performed using Model 3 (baseline Model) with randomised initial parameters to explore the proposed solution ($-2\log\mathcal{L} = -9573.75$):



- 3% of the times it is found a solution with $-2\log\mathcal{L}$ equal to -9579.12,
 - Nevertheless characterized by a large sum of fit fractions on B^- , $\Sigma FF^+ = 98.3\%$, $\Sigma FF^- = 126.7\%$.
 - Large pattern of interference is due to $K_0^{*0}(1430)$ and the non-resonant component → **overlap of broad scalar structures**.
- A second solution with essentially same NLL is found, $-2\log\mathcal{L} = -9573.73$.
 - Large pattern of interference on both, B^- , $\Sigma FF^+ = 125.1\%$, $\Sigma FF^- = 126.7\%$.

A

Component	Fit fraction (%)		Magnitude and phase coefficients				A_{CP} (%)
	B^+	B^-	a_i^+	$\delta_i^+ [^\circ]$	a_i^-	$\delta_i^- [^\circ]$	
$K^{*0}(892)$	6.0 ± 0.8	10.4 ± 1.1	0.94 ± 0.04	0 ± 0	1.06 ± 0.04	0 ± 0	12.0 ± 8.3
$K_0^{*0}(1430)$	32.6 ± 1.7	34.9 ± 2.2	2.19 ± 0.11	-85 ± 7	1.94 ± 0.11	-149 ± 5	-11.8 ± 4.4
TobiasNR_Kpi	26.9 ± 2.4	31.0 ± 2.8	1.99 ± 0.13	-164 ± 6	1.83 ± 0.12	140 ± 7	-8.2 ± 6.6
$\rho^0(1450)$	30.0 ± 1.5	32.4 ± 1.8	2.10 ± 0.11	117 ± 11	1.87 ± 0.10	77 ± 13	-11.4 ± 4.4
$f_2(1270)$	4.5 ± 0.9	10.8 ± 1.3	0.82 ± 0.09	-176 ± 12	1.08 ± 0.08	170 ± 9	27.4 ± 10.6
Rescattering	24.7 ± 1.2	6.8 ± 0.9	1.90 ± 0.09	-128 ± 13	0.86 ± 0.06	-145 ± 18	-66.1 ± 3.8
$\phi(1020)$	0.3 ± 0.2	0.4 ± 0.2	0.20 ± 0.07	-124 ± 23	0.21 ± 0.06	42 ± 30	6.0 ± 42.2
Fit Fraction Sum	125.1	126.7					

B

Component	Fit fraction (%)		Magnitude and phase coefficients				A_{CP} (%)
	B^+	B^-	a_i^+	$\delta_i^+ [^\circ]$	a_i^-	$\delta_i^- [^\circ]$	
$K^{*0}(892)$	5.7 ± 0.6	10.0 ± 1.2	0.94 ± 0.04	0 ± 0	1.06 ± 0.04	0 ± 0	12.5 ± 8.7
$K_0^{*0}(1430)$	3.5 ± 0.8	5.9 ± 1.2	0.74 ± 0.09	-176 ± 10	0.82 ± 0.09	136 ± 11	10.5 ± 14.9
TobiasNR_Kpi	30.9 ± 2.0	34.1 ± 2.5	2.19 ± 0.13	-138 ± 7	1.97 ± 0.12	166 ± 6	-10.7 ± 5.3
$\rho^0(1450)$	29.5 ± 1.5	32.4 ± 1.9	2.14 ± 0.11	-175 ± 10	1.91 ± 0.10	140 ± 13	-11.0 ± 4.4
$f_2(1270)$	4.7 ± 0.9	11.2 ± 1.3	0.85 ± 0.09	-106 ± 11	1.13 ± 0.08	-128 ± 11	27.2 ± 10.2
Rescattering	23.7 ± 1.1	6.5 ± 0.8	1.92 ± 0.09	-57 ± 12	0.86 ± 0.07	-81 ± 15	-66.7 ± 3.8
$\phi(1020)$	0.2 ± 0.2	0.4 ± 0.2	0.20 ± 0.07	-53 ± 23	0.22 ± 0.06	108 ± 33	10.1 ± 43.8
Fit Fraction Sum	98.3	100.5					

C

Component	Fit fraction (%)		Magnitude and phase coefficients				A_{CP} (%)
	B^+	B^-	a_i^+	$\delta_i^+ [^\circ]$	a_i^-	$\delta_i^- [^\circ]$	
$K^{*0}(892)$	5.7 ± 0.8	10.4 ± 1.0	0.93 ± 0.04	0 ± 0	1.07 ± 0.04	0 ± 0	14.9 ± 8.6
$K_0^{*0}(1430)$	3.5 ± 1.2	34.9 ± 3.7	0.73 ± 0.15	-176 ± 10	1.97 ± 0.14	-149 ± 3	76.1 ± 10.2
TobiasNR_Kpi	30.9 ± 1.9	31.0 ± 3.0	2.16 ± 0.13	-138 ± 7	1.86 ± 0.13	140 ± 7	-15.0 ± 5.9
$\rho^0(1450)$	29.5 ± 1.8	32.4 ± 2.1	2.11 ± 0.11	-175 ± 10	1.90 ± 0.10	77 ± 13	-10.6 ± 4.4
$f_2(1270)$	4.7 ± 0.9	10.8 ± 1.4	0.84 ± 0.09	-106 ± 11	1.10 ± 0.08	170 ± 5	25.7 ± 10.3
Rescattering	23.7 ± 1.3	6.8 ± 0.9	1.89 ± 0.09	-57 ± 12	0.87 ± 0.07	-145 ± 17	-65.0 ± 3.9
$\phi(1020)$	0.2 ± 0.2	0.4 ± 0.2	0.19 ± 0.07	-53 ± 23	0.22 ± 0.06	42 ± 30	11.2 ± 43.1
Fit Fraction Sum	98.3	126.7					

Model 3 - Solutions

- 2 $\log \mathcal{L} = -9579.12$ (**C**)

and -2 $\log \mathcal{L} = -9573.73$ (**A**) are solutions in which a large pattern of interferences between $K_0^{*0}(1430)$ and Tobias NR occurs, in B^- or in B^+ and B^- .

- Both are variations from the proposed baseline solution in which a sum of fit fractions $\sim 100\%$ is obtained.

Large and "suspicious" CP asymmetry for $K_0^{*0}(1430)$ (76%) in the -2 $\log \mathcal{L} = -9579.12$ (**C**) solution.

Large asymmetry in the interference term between $K_0^{*0}(1430)$ and Tobias NR in solution (**C**).

- The three solutions are reported in the note.

Summary/Conclusions

- We studied the $B^+ \rightarrow \pi^+ K^- K^+$ decay, which is one of the B mesons decays with larger CP asymmetry observed.
- It was found a total integrated CP asymmetry of $\sim -12\%$, and regions in the Dalitz plot with CP asymmetries up to -33% .
- The rescattering $\pi\pi \leftrightarrow KK$ region (1-1.5 GeV), presents a highest asymmetry.
 - ▶ Main focus and interesting part of our analysis.
 - ▶ We obtain a good parametrization of this region using the Peláez 2005 function but still some problems are seen near the threshold KK .
 - ▶ Several other parametrization for the rescattering region were also tested but the Peláez 2005 function provided the best description.

Summary/Conclusions

- For the $K\pi$ system:
 - ▶ $K_0^{*0}(1430)$ and the non-resonant Tobias, are broad scalar structure.
 - ▶ They can produce large pattern of interference as observe in Model 3 - solution -9573.73 and -9579.12.
 - ▶ Some tests are being performed for the total $K\pi$ S-wave.
- Overall we have a good representation of the Dalitz plot.
- Analysis still in review by the collaboration.

Backup

Classic Model

- For the construction of this model we included only known resonant states.
- Mainly Breit-Wigner and flatté lineshape were used.
- Best model chosen by lower NLL value, unless the difference in NLL is not significant when adding more resonances.

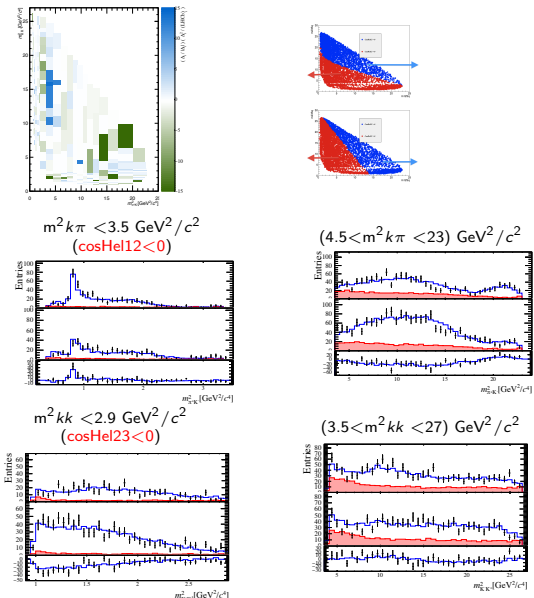
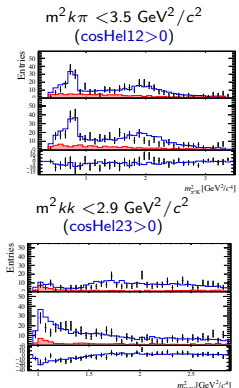
We find:

- 3 components to describe the structures on $m_{\pi^+ K^-}^2$ and 4 components for $m_{K^- K^+}^2$
- $\rho(1450)$ performs very well on parameterizing the high mass region on $m_{\pi^+ K^-}^2$ (strong pattern of interference)
- Large CP asymmetry attributed to $f_0(980)$ and $f_0(1370)$
- Both components mainly acting in the expected rescattering region.

Classic Model

Component	Fit fraction (%)		Magnitude and phase coefficients				A_{CP} (%)
	B^+	B^-	a_i^+	$\delta_i^+ [^\circ]$	a_i^-	$\delta_i^- [^\circ]$	
$K^{*0}(892)$	5.0 ± 0.7	10.5 ± 1.1	0.89 ± 0.05	0 ± 0	1.11 ± 0.05	0 ± 0	21.2 ± 8.9
$K_0^{*0}(1430)$	16.8 ± 2.1	24.8 ± 3.1	1.63 ± 0.13	-140 ± 14	1.70 ± 0.13	-148 ± 13	4.0 ± 8.9
κ	8.0 ± 1.0	10.0 ± 2.2	1.13 ± 0.10	86 ± 10	1.08 ± 0.13	31 ± 7	-4.2 ± 13.0
$\rho^0(1450)$	28.1 ± 1.5	35.8 ± 1.8	2.11 ± 0.12	-44 ± 24	2.04 ± 0.11	-30 ± 22	-3.4 ± 4.3
$f_2(1270)$	3.4 ± 0.9	9.7 ± 1.4	0.74 ± 0.10	31 ± 24	1.07 ± 0.09	60 ± 26	35.4 ± 12.8
$f_0(1370)$	5.0 ± 1.7	0.1 ± 0.2	0.89 ± 0.15	-29 ± 26	0.13 ± 0.07	-58 ± 108	-96.1 ± 7.0
$f_0(980)$	33.4 ± 2.5	11.8 ± 1.9	2.31 ± 0.14	175 ± 26	1.17 ± 0.11	-153 ± 48	-58.9 ± 5.8
Fit Fraction Sum	99.6	102.8					

Classic Model



Model 1-Improving the parametrization in $m_{\pi^+ K^-}^2$ projection

• Classic Model

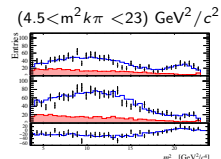
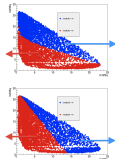
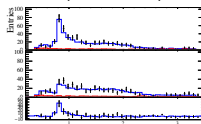
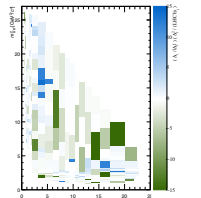
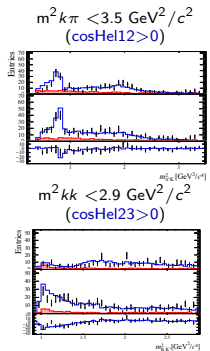
[NLL -9564] Component	Fit fraction (%)		Magnitude and phase coefficients				A_{CP} (%)
	B^+	B^-	a_i^+	$\delta_i^+ [^\circ]$	a_i^-	$\delta_i^- [^\circ]$	
$K^{*0}(892)$	5.0 ± 0.7	10.5 ± 1.1	0.89 ± 0.05	0 ± 0	1.11 ± 0.05	0 ± 0	21.2 ± 8.9
$K_0^{*0}(1430)$	16.8 ± 2.1	24.8 ± 3.1	1.63 ± 0.13	-140 ± 14	1.70 ± 0.13	-148 ± 13	4.0 ± 8.9
κ	8.0 ± 1.0	10.0 ± 2.2	1.13 ± 0.10	86 ± 10	1.08 ± 0.13	31 ± 7	-4.2 ± 13.0
$\rho^0(1450)$	28.1 ± 1.5	35.8 ± 1.8	2.11 ± 0.12	-44 ± 24	2.04 ± 0.11	-30 ± 22	-3.4 ± 4.3
$f_2(1270)$	3.4 ± 0.9	9.7 ± 1.4	0.74 ± 0.10	31 ± 24	1.07 ± 0.09	60 ± 26	35.4 ± 12.8
$f_0(1370)$	5.0 ± 1.7	0.1 ± 0.2	0.89 ± 0.15	-29 ± 26	0.13 ± 0.07	-58 ± 108	-96.1 ± 7.0
$f_0(980)$	33.4 ± 2.5	11.8 ± 1.9	2.31 ± 0.14	175 ± 26	1.17 ± 0.11	-153 ± 48	-58.9 ± 5.8
Fit Fraction Sum	99.6	102.8					

• Including the Tobias NR parametrization

[NLL -9584] Component	Fit fraction (%)		Magnitude and phase coefficients				A_{CP} (%)
	B^+	B^-	a_i^+	$\delta_i^+ [^\circ]$	a_i^-	$\delta_i^- [^\circ]$	
$K^{*0}(892)$	6.0 ± 0.8	9.9 ± 1.0	0.96 ± 0.04	0 ± 0	1.04 ± 0.04	0 ± 0	7.8 ± 8.3
$K_0^{*0}(1430)$	3.5 ± 0.8	7.0 ± 1.4	0.73 ± 0.09	-159 ± 9	0.87 ± 0.10	137 ± 11	17.7 ± 15.3
TobiasNR- $K\pi$	23.0 ± 2.0	30.0 ± 2.9	1.88 ± 0.12	-127 ± 7	1.81 ± 0.12	168 ± 5	-4.0 ± 6.7
$\rho^0(1450)$	25.7 ± 1.5	33.5 ± 2.3	1.99 ± 0.10	144 ± 20	1.91 ± 0.11	173 ± 17	-4.1 ± 4.8
$f_2(1270)$	3.2 ± 0.9	9.3 ± 1.4	0.70 ± 0.10	-139 ± 21	1.00 ± 0.08	-96 ± 20	34.0 ± 13.1
$f_0(1370)$	8.6 ± 2.8	0.7 ± 0.7	1.15 ± 0.19	162 ± 19	0.27 ± 0.13	-179 ± 74	-89.8 ± 10.3
$f_0(980)$	37.3 ± 3.2	7.8 ± 1.6	2.39 ± 0.14	-15 ± 17	0.92 ± 0.10	44 ± 39	-74.3 ± 5.2
Fit Fraction Sum	107.4	98.1					

- Introduction of Tobias NR instead of κ .
- Large interference with $K^*(1430)$ resulting on a large asymmetry.
- Overall the DP fits was improved especially on the $\pi^+ K^-$ system.
- Increase in 20 units the FCN compared to the classic model.

Including Tobias NR parametrization



Solution $-2\log\mathcal{L} = -9579.12$

Interference FF B^+	A0	A1	A2	A3	A4	A5	A6
A0	0.0568053	4.92805e-05	0.000630052	-0.0136497	-0.000706573	0.00441911	0.000239023
A1		0.0349605	0.0527508	0.0113368	-0.00395087	-0.00454856	-0.000421193
A2			0.309314	-0.0359521	-0.0169591	0.029774	-0.000291498
A3				0.295422	-1.52272e-05	3.75285e-05	-0.00608579
A4					0.0471388	2.62193e-06	-7.99387e-07
A5						0.237235	2.29388e-06
A6							0.00246504
Interference FF B^-	A0	A1	A2	A3	A4	A5	A6
A0	0.10396	0.000352452	-0.000452126	0.0109427	-0.00785348	0.000447536	0.00038089
A1		0.348916	-0.284667	-0.00324814	0.0172474	0.00239353	-0.00060458
A2			0.30966	0.00447485	-0.0258819	0.0145025	0.00053576
A3				0.323655	-5.4256e-05	2.40105e-05	0.00480291
A4					0.108116	2.74911e-06	1.57883e-06
A5						0.0681619	-1.71729e-06
A6							0.00418589
CPV Fit Fractions	A0	A1	A2	A3	A4	A5	A6
A0	0.0114507	0.000121283	-0.00055451	0.0125004	-0.00292777	-0.00235288	2.41738e-05
A1		0.128022	-0.151215	-0.00790262	0.00959617	0.0036336	-1.43199e-05
A2			-0.0465157	0.0225878	-0.00122993	-0.0109755	0.000395204
A3				-0.0325805	-1.42733e-05	-1.14009e-05	0.00554112
A4					0.0187776	-3.41545e-07	1.13032e-06
A5						-0.107572	-2.04908e-06
A6							0.000358744

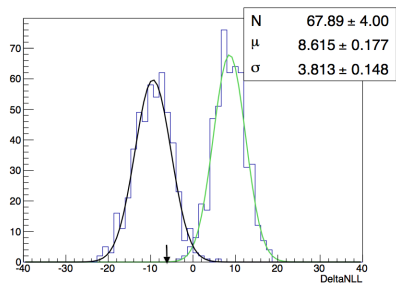
Table: Model 3: baseline solution $-2\log\mathcal{L} = -9579.12$. Interference fit fractions for B^+ , B^- and their associated CP asymmetry.

Solution $-2\log\mathcal{L} = -9573.75$

Interference FF B^+	A0	A1	A2	A3	A4	A5	A6
A0	0.056796	4.92537e-05	0.000630184	-0.0136474	-0.000708037	0.00441852	0.000238725
A1		0.034919	0.0527371	0.011333	-0.00394786	-0.0045457	-0.000420732
A2			0.309412	-0.0359212	-0.0169657	0.0297642	-0.000293173
A3				0.295408	-1.52213e-05	3.75215e-05	-0.00608468
A4					0.0471487	2.62173e-06	-7.99066e-07
A5						0.23719	2.29169e-06
A6							0.00246248
Interference FF B^-	A0	A1	A2	A3	A4	A5	A6
A0	0.0997398	-5.33565e-05	-5.73419e-06	-0.0100079	-0.00417638	0.0029366	-0.000254075
A1		0.0589703	0.0568547	0.0144407	-0.00921041	-0.00264523	0.000608532
A2			0.341299	-0.0573427	-0.0192116	0.0200081	-0.00141095
A3				0.323863	-5.38393e-05	2.34495e-05	0.00438788
A4					0.112476	2.45665e-06	1.59258e-06
A5						0.0646374	-1.70233e-06
A6							0.00412369
CPV Fit Fractions	A0	A1	A2	A3	A4	A5	A6
A0	0.00934991	-5.09874e-05	-0.000366316	0.00365156	-0.00135593	-0.00131053	-0.000245211
A1		0.00475496	-0.00642785	-0.000442024	-0.00161231	0.00150709	0.000500089
A2			-0.034447	-0.00348849	0.00167855	-0.00873235	-0.000426921
A3				-0.0337283	-1.3961e-05	-1.17575e-05	0.00536768
A4					0.0203025	-4.75801e-07	1.13438e-06
A5						-0.10965	-2.04265e-06
A6							0.000320577

Table: Model 3: baseline solution $-2\log\mathcal{L} = -9573.75$. Interference fit fractions for B^+ , B^- and their associated CP asymmetry.

Delta NLL



- Difference in the likelihood using two solutions: $-2\log\mathcal{L} = -9573.75$ and $-2\log\mathcal{L} = -9579.12$
- Not a clear separation between both curves → not real improvement of one solution respecto to the other.
- Data (arrow) in the limit of the the overlap region.

Pelaez 2005:
 $s < 950 \text{ MeV}$

$$\cot \delta_0^{(0)}(s) = \frac{s^{1/2}}{2k} \frac{M_\pi^2}{s - \frac{1}{2}z_0^2} \frac{\mu_0^2 - s}{\mu_0^2} \left\{ B_0 + B_1 \frac{\sqrt{s} - \sqrt{s_0 - s}}{\sqrt{s} + \sqrt{s_0 - s}} \right\};$$

$$B_0 = 17.4 \pm 0.5, \quad B_1 = 4.3 \pm 1.4, \quad \mu_0 = 790 \pm 21 \text{ Mev}; \quad z_0 = 195 \pm 21 \text{ Mev} \text{ [Fixed].} \quad (1)$$

where $s^{1/2} \sim 0.95 \text{ Gev.}$
 $s > 950 \text{ MeV}$ and $s < 1420 \text{ MeV}$

$$\cot \delta_0^{(0)}(s) = c_0 \frac{(s - M_s^2)(M_f^2 - s)}{M_f^2 s^{1/2}} \frac{|k_2|}{k_2^2}, \quad k_2 = \frac{\sqrt{s - 4m_K^2}}{2}; \quad (2)$$

$$\eta_0^{(0)} = 1 - \left(\epsilon_1 \frac{k_2}{s^{1/2}} + \epsilon_2 \frac{k_2^2}{s} \right) \frac{M'^2 - s}{s}. \quad (3)$$

where

$$c_0 = 1.3 \pm 0.5, \quad M_f = 1320 \pm 50 \text{ Mev}; \quad M_s = 920 \text{ Mev (fixed)};$$

$$\epsilon_1 = 2.4, \quad \epsilon_2 = -5.5; \quad M' = 1500 \text{ Mev (fixed)}. \quad (4)$$

Pelaez 2011:

It include a new interval of energy at $s_M^{1/2} = 0.85$ Gev.
 $s < 850$ MeV

$$\cot \delta_0^{(0)}(s) = \frac{s^{1/2}}{2k} \frac{M_\pi^2}{s - \frac{1}{2}z_0^2} \times \left\{ \frac{z_0^2}{M_\pi \sqrt{s}} + B_0 + B_1 w(s) + B_2 w(s)^2 + B_3 w(s)^3 \right\}, \quad (5)$$

$$w(s) = \frac{\sqrt{s} - \sqrt{s_0 - s}}{\sqrt{s} + \sqrt{s_0 - s}}, \quad s_0 = 4M_K^2. \quad (6)$$

$s > 850 \text{ MeV}$

$$\delta_0^{(0)}(s) = \begin{cases} d_0 \left(1 - \frac{|k_2|}{k_M}\right)^2 + \delta_M \frac{|k_2|}{k_M} \left(2 - \frac{|k_2|}{k_M}\right) + |k_2|(k_M - |k_2|) \left(8\delta'_M + c \frac{(k_M - |k_2|)}{M_K^3}\right), & (0.85 \text{ GeV})^2 < s < 4M_K^2 \\ d_0 + B \frac{k_2^2}{M_K^2} + C \frac{k_2^4}{M_K^4} + D \theta(s - 4M_\eta^2) \frac{k_3^2}{M_\eta^2}, & 4M_K^2 < s < (1.42 \text{ GeV})^2 \end{cases} \quad (7)$$

where $k_2 = \sqrt{s/4 - M_K^2}$, $\delta_M = \delta(s_M)$, $\delta'_M = d\delta(s_M)/ds$, and $k_M = |k_2(s_M)|$.

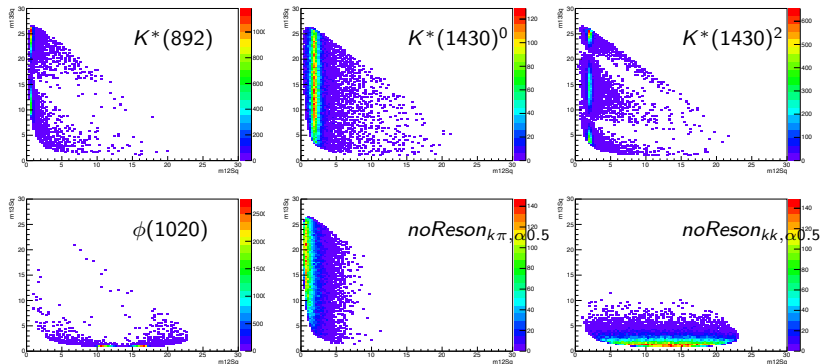
$\eta_0^{(0)} = 1$, up to the two-kaon threshold, and above that energy:

$$\eta_0^{(0)}(s) = \exp \left[\frac{-k_2(s)}{s^{1/2}} \left(\tilde{\epsilon}_1 + \tilde{\epsilon}_2 \frac{k_2}{s^{1/2}} + \tilde{\epsilon}_3 \frac{k_2^2}{s} \right)^2 - \tilde{\epsilon}_4 \theta(s - 4M_\eta^2) \frac{k_3(s)}{s^{1/2}} \right]. \quad (8)$$

The parameters obtained with the fit to data

$$\text{Resc Tobias} = \sqrt{(s/\text{sth}) - 1}/(s/\text{sth})^\alpha, \quad s = m_{kk} * m_{kk}, \quad \text{sth} = 0.493^2$$

Generating each resonance



- Non Resonant line shape:

$$A_{nr} = c_1^{nr} e^{-\alpha m_{12}^2} e^{i\delta_1^{nr}} + c_2^{nr} e^{-\alpha m_{13}^2} e^{i\delta_2^{nr}}$$

Generating each resonance

